Session

A Novel Student Laboratory on Electromagnetic Induction, Magnetic Field Measurements and Shielding

T.Bilodeau, D. Hartle , R. Jennings, and T.Dawley

Electrical Engineering Technology Department
120 Nevaldine Hall
State University of New York at Canton
Canton, NY 13617

Abstract

This paper describes a novel laboratory procedure (referred to as the Magnetic Field Effects Laboratory, or MaFEL) that enables Electrical Engineering Technology students to gain insight into Faraday's Law of Electromagnetic Induction, study AC magnetic field distributions , design electromagnetic field sensors for laboratory measurements and examine the effectiveness of various metals in shielding sensitive electronic systems against interference caused by stray magnetic fields. The prime benefit of MaFEL to engineering education is that it provides hands on learning experience in several critical areas of electromagnetics that are not covered in any other EET courses, particularly the field mapping and shielding techniques.

The implementation of the MaFEL experiment , as carried out by the students, and the correlated analysis of magnetic field measurements that were made with a hand wound solenoid probe (hereafter referred to as the " B-dot probe ") under both shielded and unshielded conditions, are discussed in this paper . In order to illustrate the nature of the experimental data and analysis that is entailed by MaFEL , several graphs of magnetic field intensity that were measured with the B dot probe along the axis of a wire loop carrying an AC current of variable frequency are presented and their significance is discussed . In addition, the effects of enclosing the B-dot probe inside a cylindrical shield made of high permeability metal on the probe's detection sensitivity are noted in order to illustrate the fundamental concepts of shielding low frequency magnetic fields .

In closing, some potential industrial applications where the students can apply the knowledge and skills they derived from their MaFEL laboratory experience to solve practical electromagnetic systems design , interference and shielding problems are discussed and future plans for the continued development of the MaFEL procedure are noted.

I. Introduction

The ability to visualize the low frequency AC magnetic field distributions that occur in the vicinity of 60 Hz AC electric power generation and transmission equipment , such as transformers, rotational machines, switchgear and cable ; and to understand the physical factors that determine these fields ; are very important skills for an electrical engineering technician (EET) to have. This understanding of AC magnetic field behavior enables an EET to identify the most probable locations in an electrical system topography where undesired electromagnetic interference (EMI) may be inductively coupled from

Copyright @ 2005 , American Society for Engineering Education "

60 Hz AC powered equipment to EMI sensitive electronic devices, particularly the desktop computers , networked LAN stations, laptops, and other digital computer peripherals that are now so common in the industrial , laboratory and office environments . Also, it should be mentioned at this point that EMI produced by many 120 VAC line powered equipment often can encompass a fairly wide spectrum of frequencies extending from 60 Hz and their associated low order harmonics up to radio frequency hash of several MHz (with the latter emanating from such common sources as inductive ballasts in fluorescent lights , rotating electrical machines or switch mode power supplies) [2].

This paper describes a new EET student laboratory procedure regarding magnetic field analysis that was conceived at SUNY Canton for senior level EET students taking the Electrical Power and Machines course. This new procedure will be hereafter referred to as the Magnetic Fields Effects Laboratory procedure , or MaFEL. By carrying out the calculations and measurements specified in MaFEL, the students can gain insight into Faraday's Law of electromagnetic induction, measurement techniques for AC magnetic fields and EMI shielding techniques .

The key impact of MaFEL on the education of EET students is that it enables the students to gain insight into several critical aspects of electromagnetism (i.e. field measurements and low frequency magnetic flux shielding) that are not discussed in any other course in the EET curriculum. The practical experience derived from MaFEL can be readily applied by the EET students at SUNY Canton to many of the laboratory measurements they perform in their two semester course on Electrical Power and Machinery .

The procedures carried out in the execution of the MaFEL laboratory include the use of fundamental electromagnetic theory (e.g. Ampere's and Biot-Savart Laws) to deduce magnetic field distributions near simple AC conductor geometries, design and construct a solenoidal dB/dt sensing probe (the " B-dot probe") to measure the AC voltages induced by the magnetic fields, compute a calibration factor for the probe and then use it to map out the field intensity along the axis of a circular shaped wire loop that carries an AC current of variable frequency . Graphs of the measured field magnitudes versus axial distance that were compiled by the students are presented in section IV of this paper .

To verify the accuracy of their B-dot probe, the students repeated the field measurements with a commercial field sensor and checked for correlation among the two data sets . In addition, the students measured magnetic field intensities when the B-dot and commercial probes were shielded with two different types of high permeability metals. The students then calculated the attendant attenuation factors provided by the shields. The analysis of shielding effects was done over a 3 kHz to 600 kHz range in order to investigate the variation of shield effectiveness with respect to frequency .

In sum, the MaFEL procedure provided the EET students with valuable hands on experience in the measurement of the AC magnetic fields that are produced by typical AC line powered equipment and appliances, and in the methods of shielding sensitive electronic systems from spurious voltages that can be inductively coupled from nearby stray magnetic fields.

The MaFEL laboratory set-up and procedure, along with the corresponding electromagnetic theory, field measurement and shielding techniques , are described in the Experimental Implementation section of this paper. Several samples of real data plots

Copyright @ 2005 , American Society for Engineering Education "

of the measured axial magnetic field distributions and shielding effectiveness that were obtained by the students when performing axial magnetic field measurements on a circular wire loop that was carrying an AC current of variable frequency (from 1 to 600 kHz) are also presented in the Experimental Results section in order to illustrate the typical numerical data that are obtained when students perform the MaFEL exercises.

As mentioned above , the data provided by the B-dot sensor is also compared to that obtained with a commercial magnetic field probe for both shielded and unshielded conditions. In closing , a summary of the B-dot probe's diagnostic capabilities and the ability of the student fabricated shields to attenuate spurious low frequency AC magnetic fields is presented and potential applications of the MaFEL concepts to solving EMI problems in real industrial settings are noted.

II. Experimental Implementation

The MaFEL experiment was carried out by using a solenoid search coil, which was designed , constructed and calibrated by the students as part of the experimental procedure, to measured the intensity of the magnetic fields that were produced by an AC sinusoidal current that was flowing through a circular loop of wire. The experimental set-up is shown in Figure 1 and the corresponding equipment specifications appear in Table 1 . Note that a more detailed sketch of the B-dot probe's physical structure is also shown in Figure 3 , which appears in the next section.

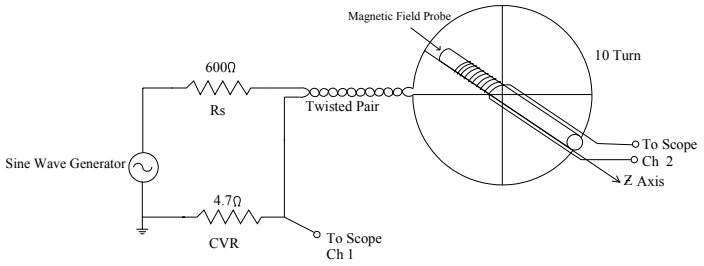

Figure 1. Block diagram of MaFEL experiment (Equipment specifications listed in Table 1)

Table 1. Specifications for equipment used in the MaFEL experiment.

- Hewlett Packard 54600B Digital Storage Oscilloscope (100MHz bandwidth)
- Hewlett Packard 200CD Sinewave Generator
  Output Resistance : 600 Ohms
  Frequency Range : 10 Hz to 600 kHz
  Short Circuit Current : 200 mA AC
- Wire Loop - 10 turns, 15 cm diameter (AWG 16 stranded wire)
- Current Viewing Resistor (CVR) – 4.75 Ohm, 1 %,¼ W Carbon Film Resistor
- Magnetic Field Sensing Coil -
  B-dot solenoid probe (see text and Figure 2 for specifications)
  Magnetic Shield / Perfection Mica EP-101A Magnetic Field Probe
  (see text and Table 2 for specifications on the EP-101A probe)

Copyright @ 2005 , American Society for Engineering Education "

As illustrated in Figure 1, the solenoid probe was used to measure the magnetic field along the center axis of the wire loop . The loop (15 cm in diameter) was energized by a Hewlett Packard 200 CD vacuum tube oscillator, which was chosen because of its capability to drive up to 200 mA AC current into a short circuit (i.e. the wire loop was essentially a short circuit load, with a calculated DC resistance of 0.044 Ohms) [1]. The tube oscillator also provided a high quality sinusoidal output voltage waveform over the range of frequencies (1 to 600 kHz) used in the experiment. A wood meter stick was fixed at the center of the wire loop in order to provide a longitudinal axis , upon which the magnetic field sensing coils could be conveniently placed to measure the corresponding field magnitudes at various points along the central axis (i.e. z axis) of the loop.

Before conducting the magnetic field measurements along the loop's longitudinal z axis, the students first had to design a solenoid field probe (the "B-dot probe ") and calibrate it . The key design features of the field probe are explained below.

The students were required to design a solenoid coil that could sense AC magnetic fields by means of the corresponding sinusoidal voltage induced across the coils' output leads. The solenoid characteristics were based on Faraday's Law of Electromagnetic Induction, which states that the voltage induced across a conductor coil that is perpendicular to a time changing magnetic field is given by

$$E = N \, d\Phi/dT$$

where N is the number of coil turns and $d\Phi/dT$ is the first derivative of the AC magnetic flux passing through the coil with respect to time . [1] For a sinusoidal field of crest (i.e..zero to peak) value B , the time derivative is just the crest value scaled by the radian frequency w ,

$$B(t) = B \sin(wt) \qquad (1)$$

$$dB(t)/dT = wB \cos(wt) \qquad (2)$$

The corresponding voltage induced in a coil of N turns is given by

$$E = NAwB \cos(wt) \qquad (3)$$

where N is the number of coil turns and A denotes the cross section area enclosed by the coil. [1] Inspection of Eqn (3) shows that the induced coil voltage will increase linearly with respect to the frequency of the AC magnetic field. Note that this linearity between field amplitude and induced coil voltage would not hold if the coil were wound around a ferromagnetic core, due to core saturation and the variance of permeability with frequency. [1,2]

However, the B-dot probe designed by the students avoids this problem by utilizing an air core coil that responds linearly to fields over a wide frequency range. The only factor limiting the linearity of the B-dot coil was the resonance of the coil inductance with its stray winding capacitance, which was empirically observed for

Copyright @ 2005 , American Society for Engineering Education "

frequencies in the 250 to 400 kHz band (and in agreement with the estimates of 450 uH and 250 pF or coil inductance and interwinding capacitance, as will be explained later in this section). To avoid possible inaccuracies, the B-dot sensor was not used by the students to measure any AC fields in empirically observed B-dot coil resonance range of 250 to 400 kHz.

The next step for the students in their probe design was to estimate the magnitude of the magnetic field at the center of the wire loop (i.e. $z = 0$). In reference to the loop depicted in Figure 2, the field at $z = 0$ can be estimated by using the Biot-Savart Law .

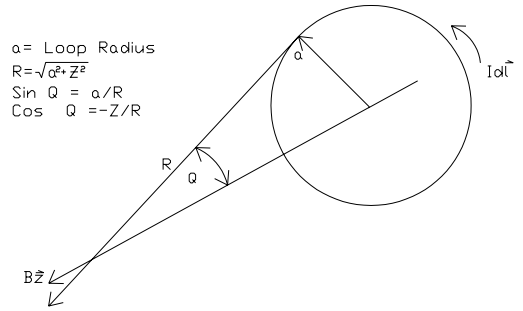

Figure 2. Use of the Biot-Savart Law to calculate the axial magnetic field along the longitudinal axis of a wire loop carrying an elemental current IdL [1].

The Biot-Savart Law states that the field at a distance R from a circular loop of wire is given by [1]

$$B = \mu I \sin Q * dL / 2 R^2 \qquad (4)$$

where u is the magnetic permeability for air (i.e. $\mu = 1.256$ uH/m), dL denotes the elemental distance along the wire loop circumference, R is the diagonal distance from dL to a point along the loop center z axis, and Q is the angle between distance vector R and the z axis. Eqn (4) can be simplified by substituting relations (5) and (6) given below , for R and sin Q respectively . Eqn.s (5) and (6) are then used to obtain Eqn (7), the final expression for the the axial magnetic field, as a function of z, the displacement along the z axis. [1]

$$R = (a^2 + z^2)^{0.5} \qquad (5)$$

$$\sin Q = a / (a^2 + z^2)^{0.5} \qquad (6)$$

$$B(z) = u I a^2 / 2(a^2 + z^2)^{1.5} \qquad (7)$$

Eqn (7) gives the magnetic field amplitude along the center axis of a circular wire loop that is carrying a current I . [1] To determine the field intensity at the loop's center point, we set $z = 0$ in Eqn (7) to obtain

$$B(0) = \mu I / 2a \qquad (8)$$

Copyright @ 2005 , American Society for Engineering Education "

It can also be shown that the axial field for a short multi-turn solenoid whose axial length is much shorter than its radius is expressed by

$$B(z) = \mu N I a^2 / 2(a^2 + z^2)^{1.5} \qquad (9)$$

and the field far from the loop center along the z axis is approximately (i.e. neglecting the relatively low value of a in the denominator) given by [1]

$$B(z) = \mu I a^2 / 2 z^3 \qquad (10)$$

In the MaFEL procedure, the students compute the magnetic field strength at the center of the wire loop by using Eqn (8) , with the radius a set equal to 7.5 cm , N set equal to 10 turns and the AC crest current I set equal to 125 mA. Inserting these values into Eqn (8) gives a peak center field of 10.5 uT, a typical field level for the AC loop currents used in the MaFEL experiment.

After the students had determined the center field for the wire loop, they needed to design the physical and electrical parameters of the solenoid sense coil . The students were instructed to design a coil that would have an induced voltage of 100 mV peak when a 1 kHz AC current of 100 mA peak was flowing through the loop. The coil form consisted of a cylindrical wood dowel that was 29 cm long and 1.5 cm in diameter. A schematic diagram illustrating the mechanical construction of the B-dot probe is shown in Figure 3

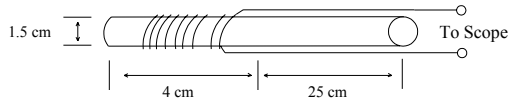

Figure 3. Mechanical schematic of the B-dot probe's construction.

The students evaluated Eqn (2) for the number of coil turns with the induced coil voltage E set to 100 mV, the radian frequency w set to 6140 rad/s , the crest field B set to 10 uT and coil cross section area A set to 4.9 cm^2 (i.e. the cross sectional area of the wood dowel) , and the computed result was approximately 500 turns. The students then wound the solenoid search coil with 500 turns of AWG 30 magnet wire (enamel insulated). The 500 turns encompassed a linear distance of 5 cm, with two layers of overlapping turns. The stray capacitance of this solenoid coil resonated with its winding inductance to yield a resonant frequency in the 250 to 400 kHz band that was measured by the students when first calibrating the B-dot probe (i.e. a total of 8 probes were made, and all had resonance somewhere in the 250 – 400 kHz range). This parasitic resonance was also estimated to be about 320 kHz , based on approximate calculations of coil inductance (i.e. 400 uH) and winding capacitance (i.e. 250 pF) that were derived from published formulas in the Radio Engineer's Handbook. [3]

The final step in the design of the B -dot probe was to calibrate its field detection sensitivity. This was accomplished by using the theoretical formula given by Eqn (8) to calculate the center loop field for a 1 kHz AC current of 125 mA peak ; and then

Copyright @ 2005 , American Society for Engineering Education "

dividing this theoretical value by the voltage that was measured across the probe leads when it was placed at the wire loop's center. This yielded a calibration factor of 1.10 uT/ mV (i.e. typical value obtained by the students) that was subsequently used for all axial measurements made at a frequency of 1 kHz. The B-dot probe was re-calibrated for each of the loop current frequencies that were used in the MaFEL procedure (i.e. 3, 10, 30, 100 , 200 and 600 kHz), but negligible differences in the probe sensitivity as a function of frequency were found (as should be expected for an air core solenoid). The only exceptions were observed when the B-dot probe was used to measure AC fields within the 250 to 400 kHz resonance band, so this range was not included in the MaFEL experiment because the probe's calibration factor was not intended to compensate for the often unpredictable effects of parasitic LC resonance . [3]

Another important factor affecting the MaFEL procedure was the frequency range of the AC loop currents , which was between 1 and 600 kHz. The lower end of the range was chosen because the minimum reliable detection sensitivity for the B-dot probe was approximately 2.5 uT for a field frequency of 3 kHz. Therefore any lower frequency field would require a proportionately higher intensity in order to be detected by the B-dot probe (e.g. the minimum detection threshold of the B-dot probe for a 60 Hz magnetic field would be about 750 uT) . Since the AC sinewave generator and wire loop used in the MaFEL experiment could only produce a maximum field of 10 uT at 3 kHz, lower frequencies were not employed. Note, however, that the B-dot probe is capable of making field measurements for 60 Hz AC frequencies , as long as the minimum field amplitude exceeds the 750 uT threshold .

After the students had successfully designed, constructed and calibrated their B-dot sensing coil, they were then ready to tackle the next step of the MaFEL experimental procedure, which was to measure the magnetic field produced by the wire loop as a function of axial distance (as measured from loop center) for 125 mA AC loop currents of variable frequency. The data obtained from the B-dot probe measurements are described in the next section.

III. Presentation of Experimental Results

The students measured the axial magnetic field distribution produced by the 125 mA AC current flowing through the 15 cm diameter wire loop by moving the B-dot coil to various positions along the center axis of the loop. The AC loop current was monitored during these field measurements by using a 4.7 Ohm precision resistor in the ground return lead of the sinewave generator, as was shown in Figure 1. The 600 Ohm internal resistance of the function generator ensured that the loop current magnitude remained constant throughout the experiment, because the loading effects of the current viewing resistor and small fluctuations in the loop wire resistance (due to the skin effect at higher oscillator frequencies) was swamped out by the comparatively large source resistance of 600 Ohms.

The students recorded the magnetic field strength along the loop axis over a range of 0 to 30 cm, and then made plots of the magnetic field intensity versus axial distance z in order to provide a visual representation of the measured fields . These plots appear in Figure 4 , parts a through g, for frequencies of 1 , 3, 10, 30 , 100 , 200 and 600 kHz ,

Copyright @ 2005 , American Society for Engineering Education "

respectively . Note that the students also repeated the measurements of the axial fields with a commercial magnetic pick up coil (i.e. the EP-101A probe referred to in Table 2), and these field values are also graphed along side the B-dot probe values in Figure 4 , parts b,c and d ; in order to facilitate comparisons. The B-dot probe was not used to measure fields whose frequency was less than 3 kHz due to sensitivity limitations as explained in section II (i.e. insufficient signal voltage induced in the coil below 3 kHz)and the commercial EP-101A sensor was not used at frequencies above 10 kHz due to bandwidth limitations. [2]

Inspection of the field curves in Figure 4 b,c and d reveals that the two probes yielded similar data, with the B-dot probe indicating slightly higher intensities. This small difference can be attributed to the specified 10 to 3000 Hz range of the PM probe, with an attendant -3 dB per octave roll off in sensitivity (empirically observed) that occurred as the field frequency increased beyond 1 kHz (for this reason, the PM sensor was not used for field mapping above 10 kHz). [2]

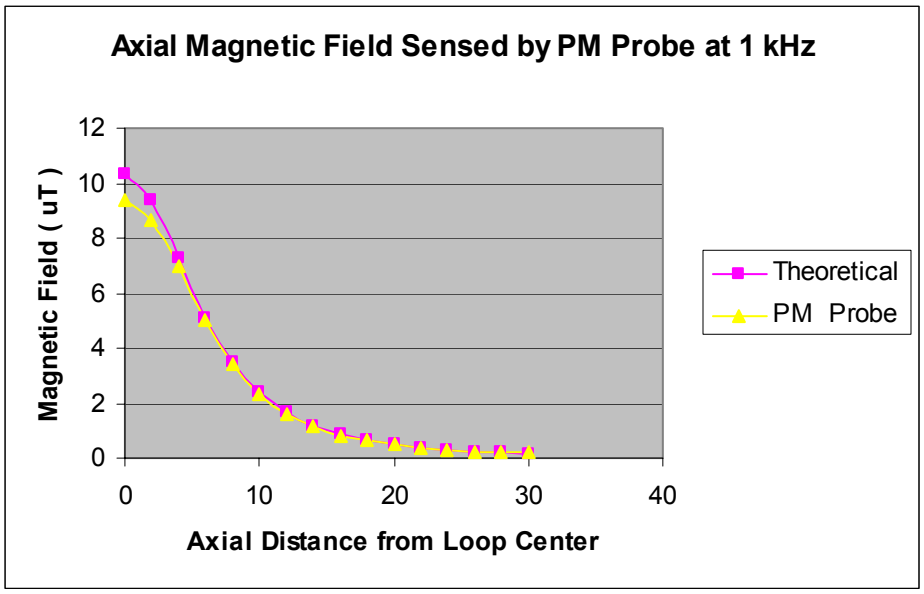

Fig. 4a

"Proceedings of the 2005 American Society of Engineering Education Annual Conference & Exposition Copyright @ 2005 , American Society for Engineering Education "

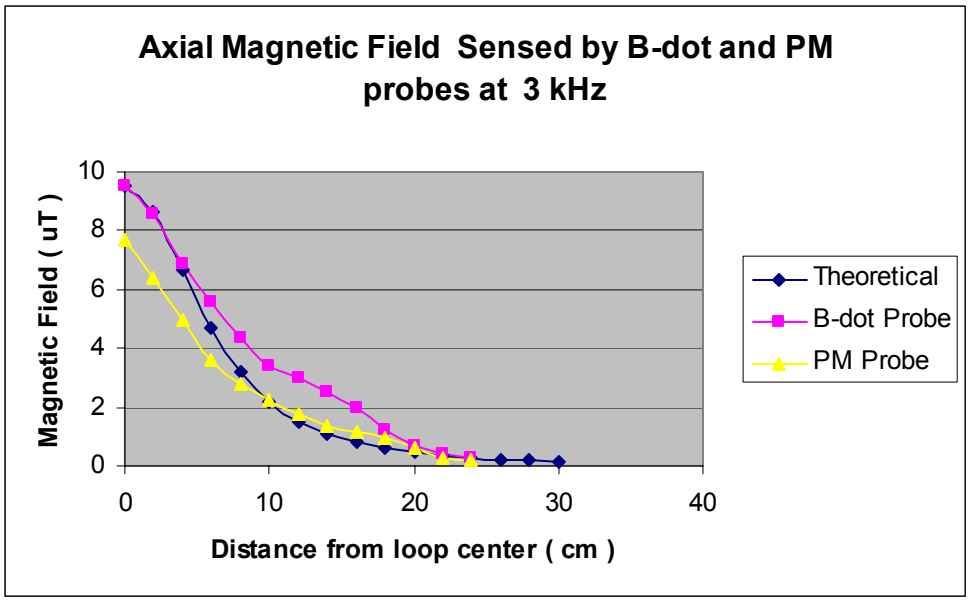

Fig.4b

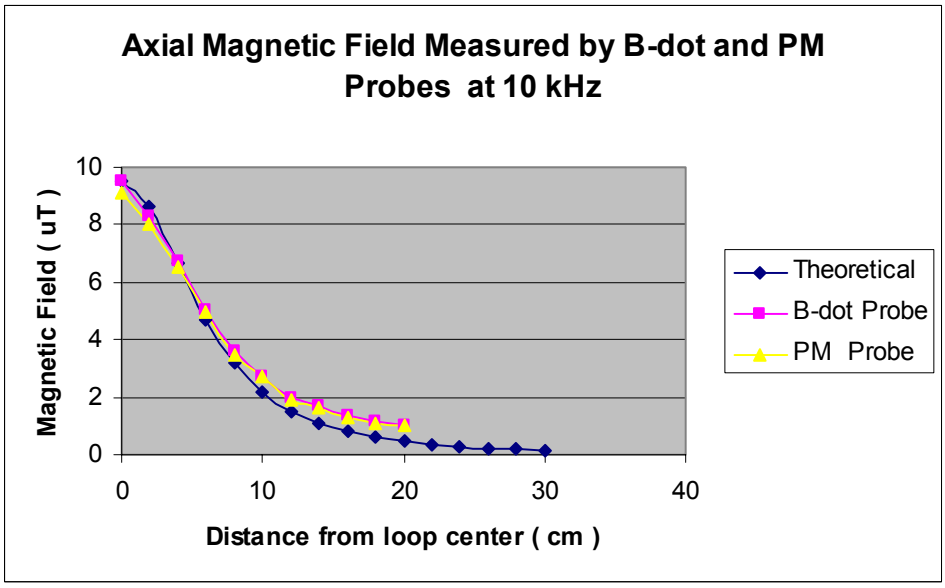

Fig.4c

"Proceedings of the 2005 American Society of Engineering Education Annual Conference & Exposition Copyright @ 2005 , American Society for Engineering Education "

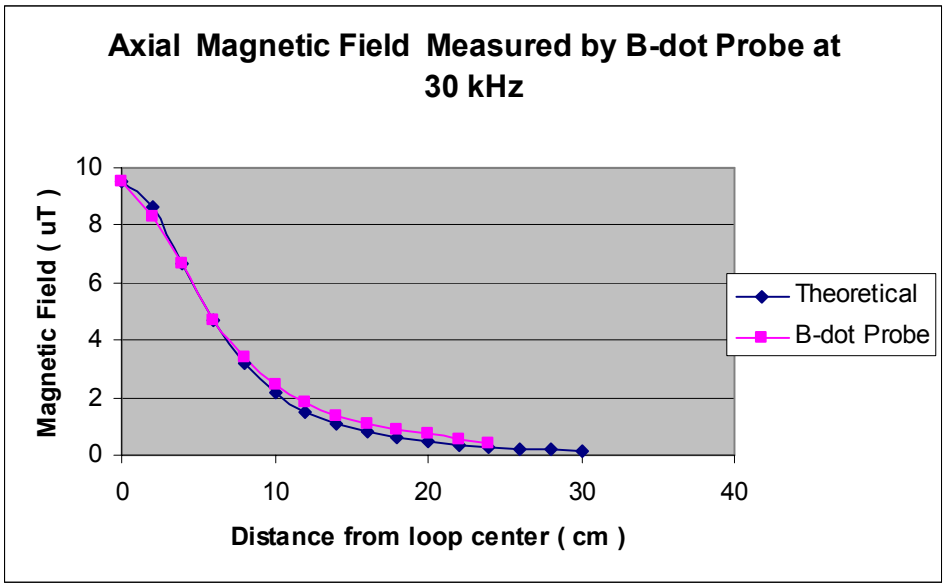

Fig.4d

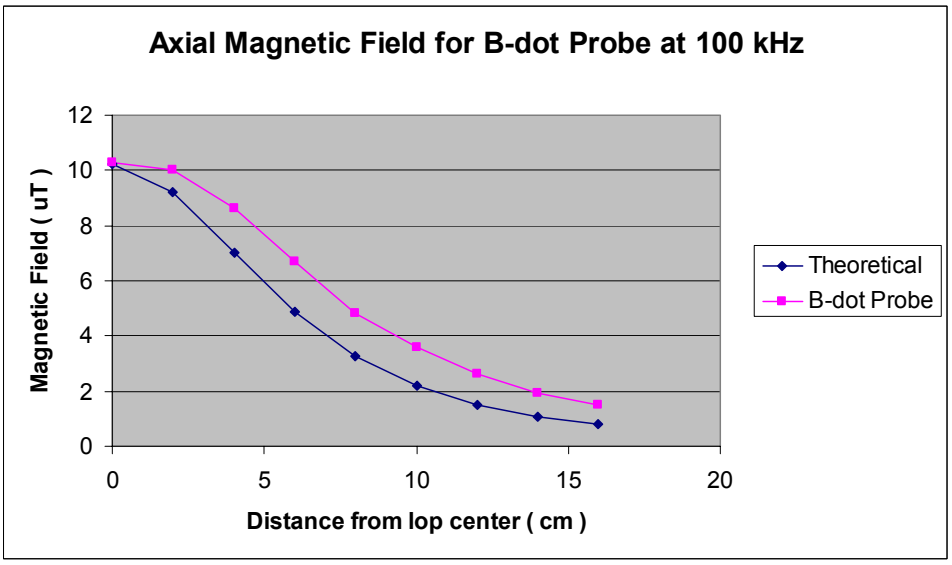

Fig.4e

"Proceedings of the 2005 American Society of Engineering Education Annual Conference & Exposition Copyright @ 2005 , American Society for Engineering Education "

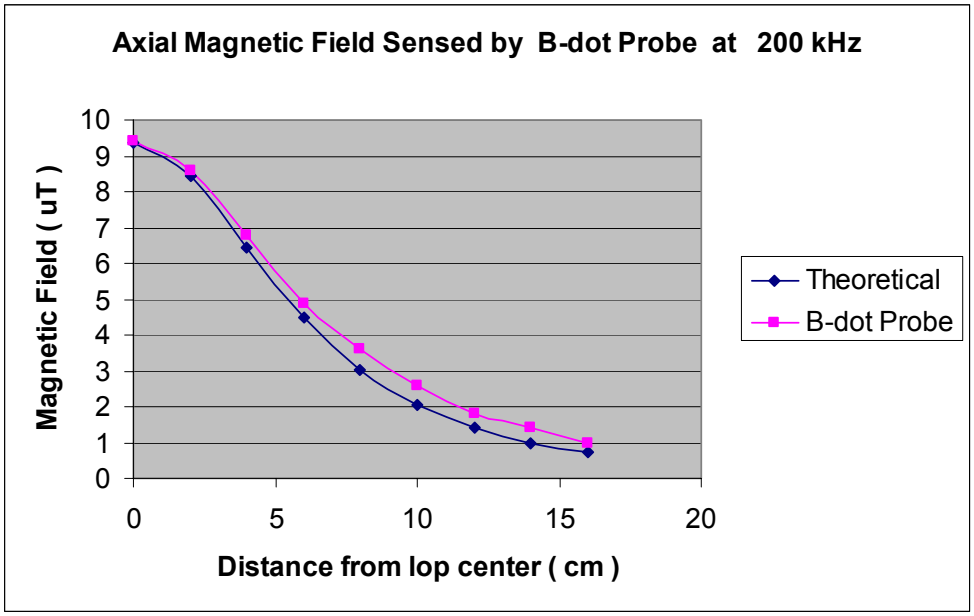

Fig.4f

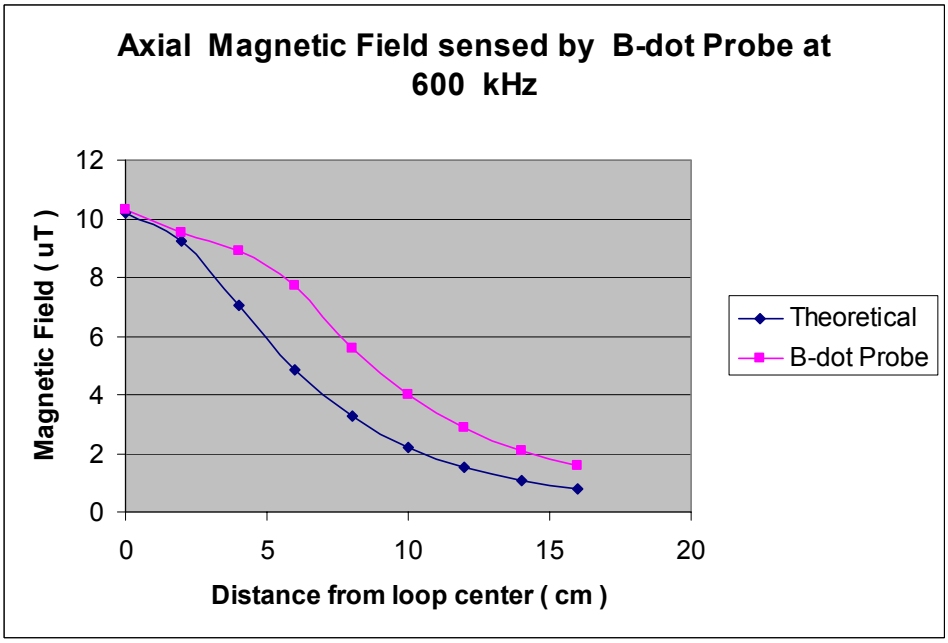

Fig.4g

Figure 4. The magnetic field intensity along the longitudinal axis of the wire loop, as measured by the B-dot and PM magnetic pick up coils, at frequencies of 1 kHz, 3 kHz , 10 kHz , 30 kHz , 100 kHz , 200 kHz and 600 kHz . The theoretical field intensities computed from Eqn (7) are also graphed to allow for comparison.

The commercial field sensor was the EP-101A Magnetic Field Pick-up Probe manufactured by the Magnetic Shield / Perfection Mica Company ; which is generally

Copyright @ 2005 , American Society for Engineering Education "

referred to in this paper as the " PM probe "[2]. The specifications for this magnetic field sensing coil are listed in Table 2.

Table 2 . Specifications for the EP-101A Magnetic Field Pick-up Probe [2]

Nominal sensitivity : 20 mV per Gauss at 60 Hz
Frequency range : 10 Hz to 3000 Hz

Note that the PM probe utilizes a ferromagnetic core, and thus it cannot be used for reliable measurements beyond the core's maximum frequency limit of 3 kHz (although it can be used for relative measurements well above 3 kHz). [2] This upper frequency limit of the PM probe should not be interpreted as a drawback, because the PM probe was designed to have maximum sensitivity for 60 Hz fields and their primary harmonics, and it is a very valuable instrument for analyzing EMI problems and shielding designs for electronic systems located in environments with adverse 60 Hz AC magnetic fields .

After the initial magnetic field data was obtained with the B-dot and PM probes, the students then investigated the effects of two shielding metals on the probes' sensitivity. This experimental investigation of magnetic field shielding was carried out by inserting the B-dot and PM probes into two cylindrical shields made from two high permeability metals, which are referred to as the co-netic and netic alloys, that were obtained from the Magnetic Shield / Perfection Mica Company . [2] The important electrical and mechanical properties of the shielding alloys are given in Table 3 and representative B-H curves are shown in Figure 5.

Table 3. Critical Properties of the Netic and Co-netic Shielding Metal Alloys that were obtained from the Magnetic Shield / Perfection Mica Company . [2]

	Co-Netic	Netic
Initial permeability	30000 u	200 u
Maximum permeability *	450000 u	4000 u
Resistivity (uOhm-cm)	55	11
Conductivity (S/cm)	1818	9090
Saturation Flux Density	0.8 T	2.14 T
Skin Depth at 1 kHz	680 um	3700 um
Specific gravity	8.74	7.86
Elasticity Modulus	25000 psi	30000 psi
Melting Point	2650 'F	2790 'F

* u = 1.256 uH/m , the permeability of air

Copyright @ 2005 , American Society for Engineering Education "

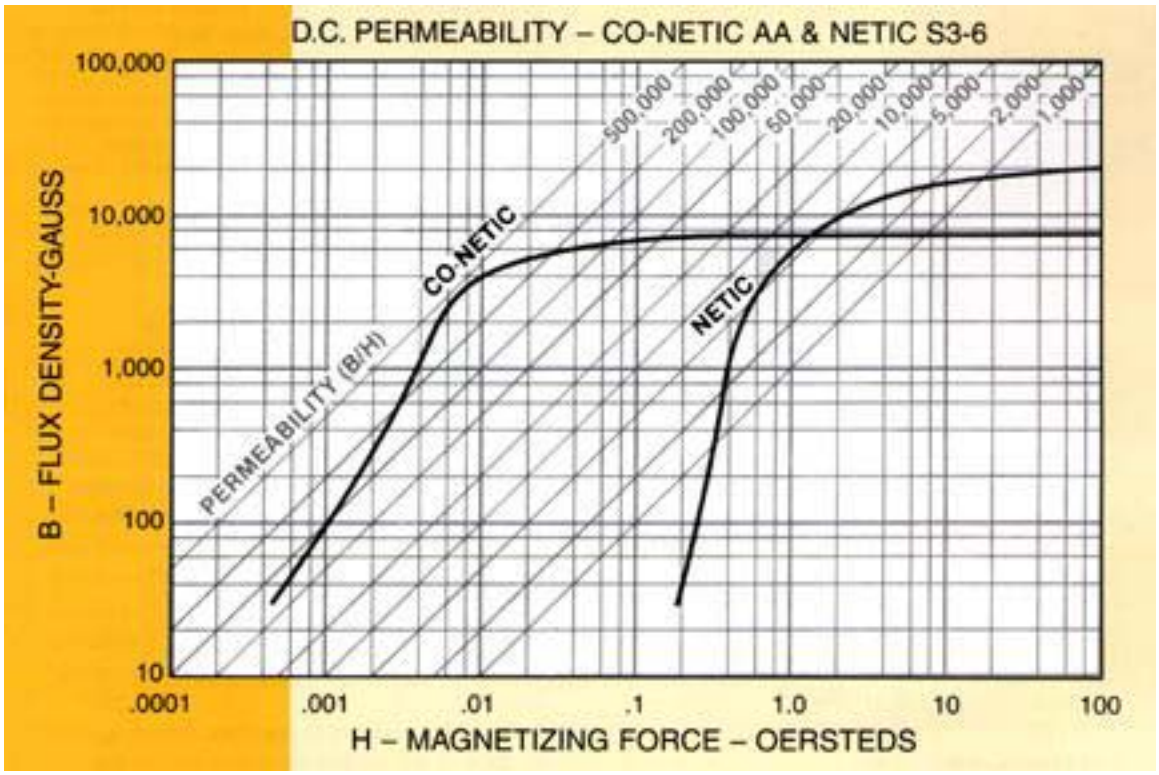

Figure 5 . Manufacturer's published B-H magnetization curves for the netic and co-netic alloys when subjected to DC fields. Note that the above data is proprietary to the Perfection Mica / Magnetic Shield Company [2].

The netic and co-netic alloys are used for shielding against DC and low frequency AC fields because they provide a high permeability, low reluctance path for the incident magnetic flux lines (i.e. the magnetic field generated by an external source of EMI) to be confined in, and thus the flux lines are diverted away from the electronic system that is being shielded. [2] The netic metal offers superior shielding against fields of high magnitude, due to its high saturation flux of 2.1 T . The co-netic material provides better shielding at low frequencies (compared to netic) due to its high initial relative permeability of 30000 (Note that this quoted value of permeability corresponds to DC and low frequency AC fields) . [2]

The EET students constructed their own shields when performing the MaFEL procedure shields by wrapping thin sheets (0.004 inches , or 4 mil thick) of the netic and co-netic metals around cylindrical sections of PVC pipe (the PVC tube was 10 cm long, 3.8 cm outer diameter and 3.5 cm inner diameter) . One end of the cylindrical shields was covered by a circular cut out of the shielding metal to create a " tin can " type of shielded enclosure ; in which either the B-dot or PM probes could be inserted into in order for the EET students to perform the MaFEL measurements of shielded magnetic fields along the axis of the wire loop.

The students used the shielded B-dot and PM probes to repeat their measurements of the axial field produced by the wire loop at various frequencies. The corresponding field intensities that were measured with the shielded probes at frequencies of 1, 3,10, 30 , 100 , 200 and 600 kHz were then graphed by the students so that they could be compared to the amplitudes of the original unshielded fields . The plots of the attenuated axial fields

Copyright @ 2005 , American Society for Engineering Education "

are shown in Figure 6 , parts a,b,c,d,e,f , g and h ; and they will be analyzed in the next section of this paper to permit comparison of the effectiveness of the co-netic and netic alloys as magnetic shields for AC fields encompassing the 1 to 600 kHz range.

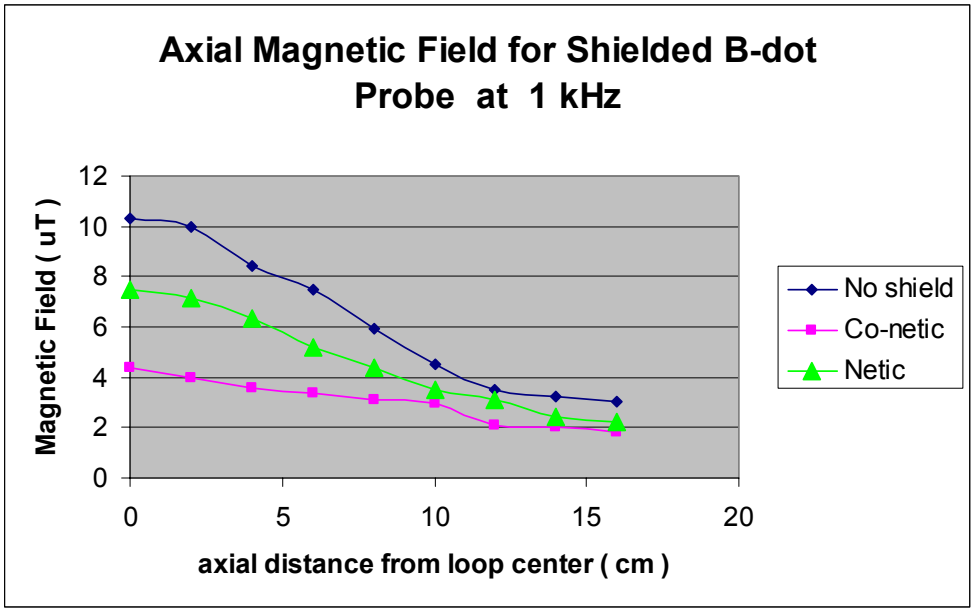

Fig. 6a

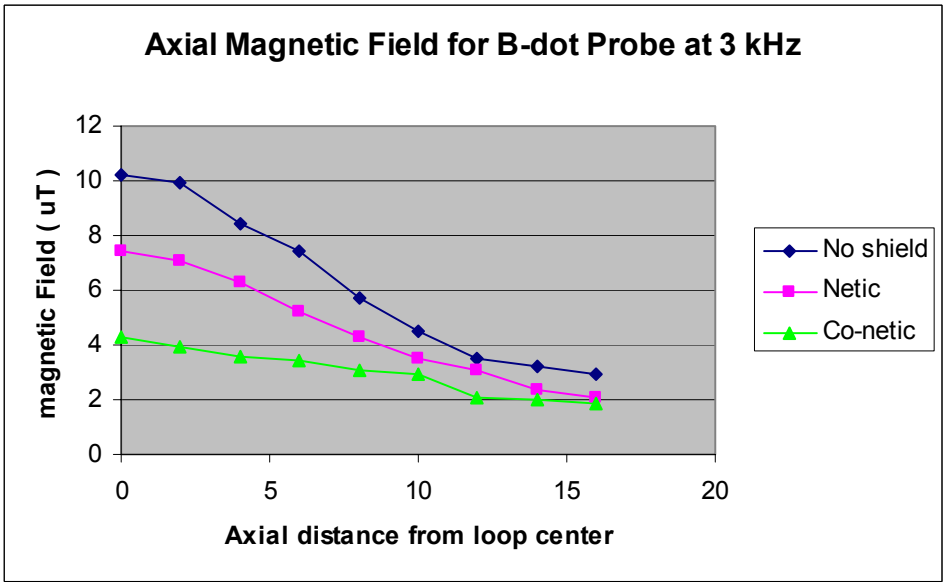

Fig.6b

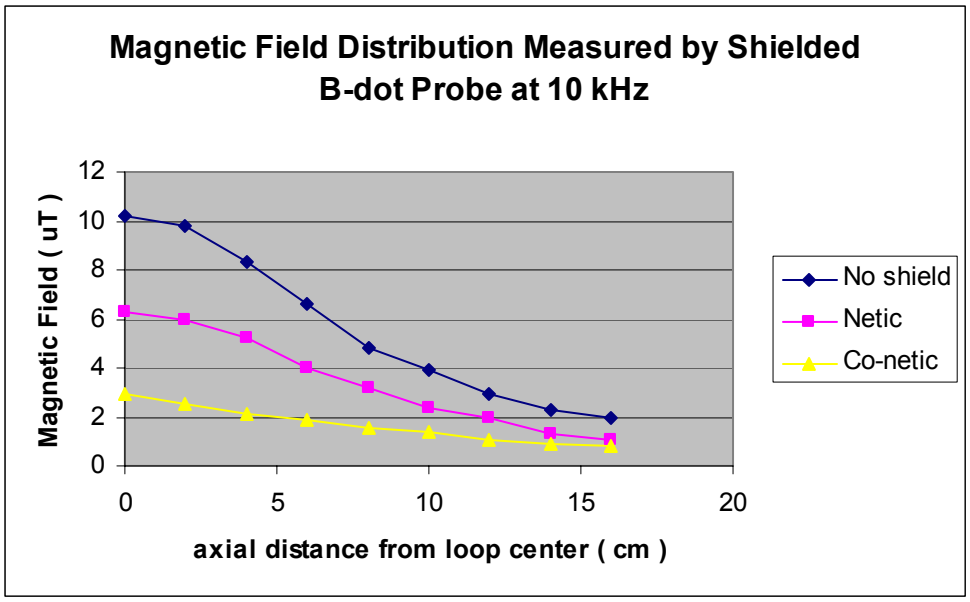

Fig. 6c

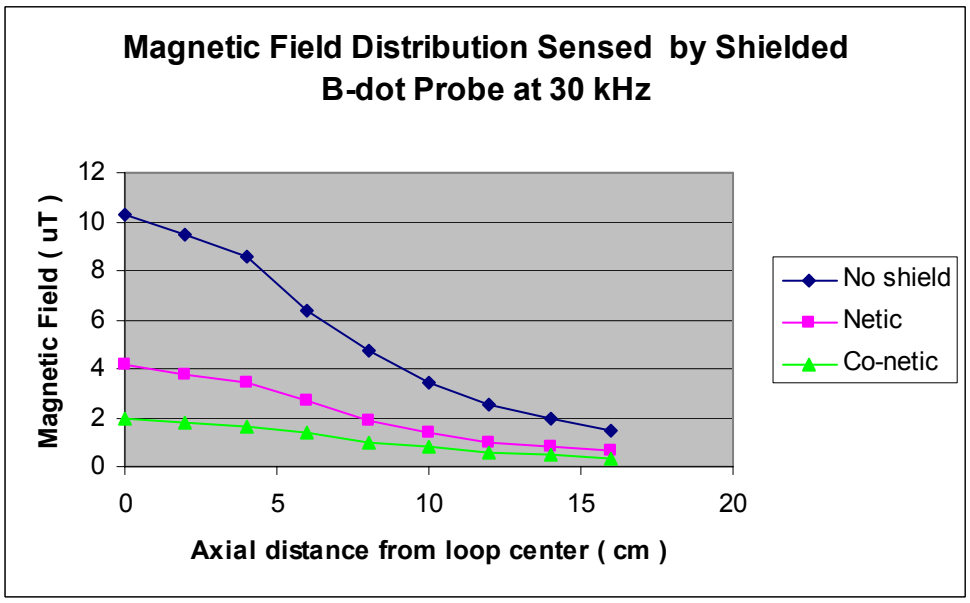

Fig. 6d

"Proceedings of the 2005 American Society of Engineering Education Annual Conference & Exposition Copyright @ 2005 , American Society for Engineering Education "

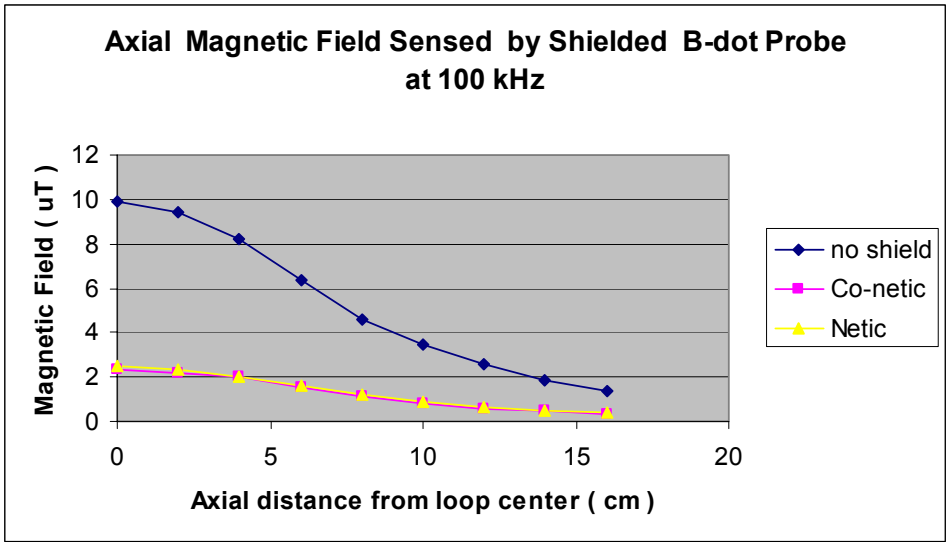
Axial Magnetic Field Sensed by Shielded B-dot Probe at 100 kHz
Magnetic Field (uT)
12
10
8
6
4
2
0
0
5
10
15
20
Axial distance from loop center (cm)
no shield
Co-netic
Netic

Fig. 6e

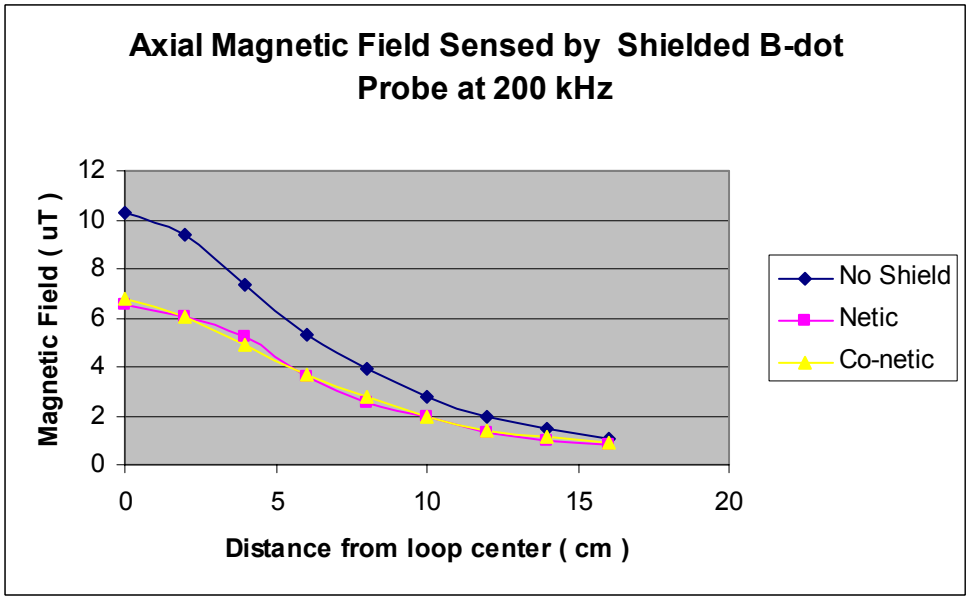
Axial Magnetic Field Sensed by Shielded B-dot Probe at 200 kHz
Magnetic Field (uT)
12
10
8
6
4
2
0
0
5
10
15
20
Distance from loop center (cm)
No Shield
Netic
Co-netic

Fig. 6f

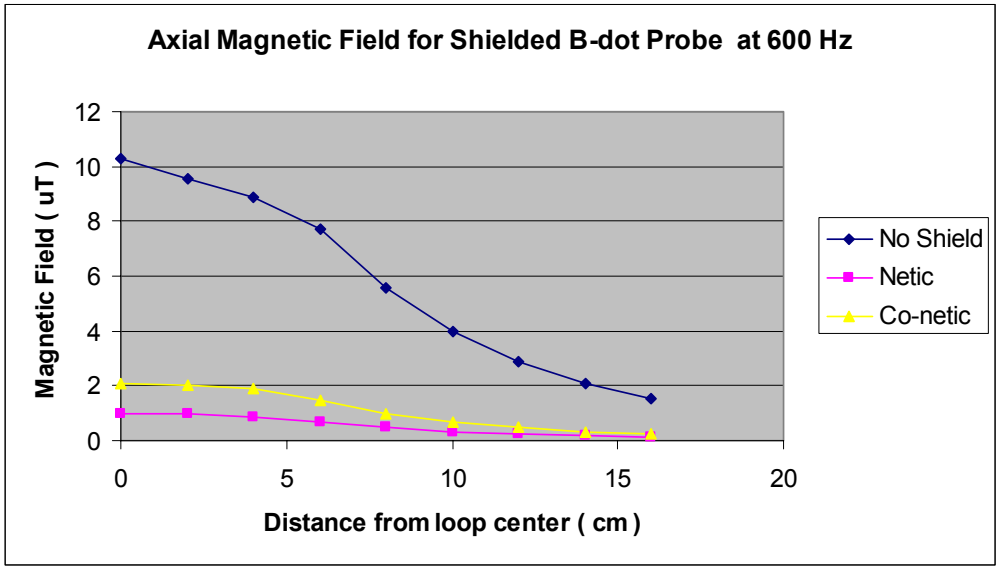

Fig. 6g

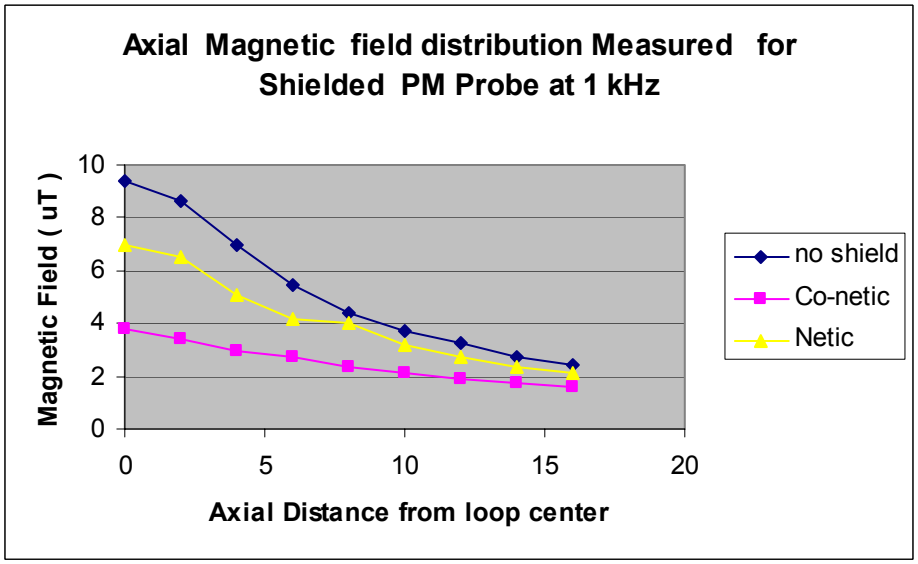

Fig. 6h

Figure 6. Plots of the axial magnetic field intensities measured by the unshielded and shielded B-dot and PM probes at frequencies of 1 kHz , 3 kHz , 10 kHz , 30 kHz , 100 kHz , 200 kHz and 600 kHz. The field levels recorded for the unshielded probes (as seen in Figure 4) are also graphed to allow for comparison.

Before departing this section, it should be pointed out that one of the most outstanding features of the shielded data corresponds to that graphed in Figure 6 e , f and g . These plots show the merging of the attenuated magnetic field curves measured for the two alloys at frequencies of 100 and 200 kHz (i.e. the attenuation factors become approximately equal at these frequencies , so the field intensity curves essentially overlap each other) . Examination of Figure 6 a,b,c and d reveals that the co- netic shield provided

Copyright @ 2005 , American Society for Engineering Education "

about twice as much attenuation as did the netic shield at the lower frequencies (i.e. at 30 kHz and below), but at the higher frequencies of 100 and 200 kHz the attenuation provided by both shields was roughly equal (as seen in Figures 6 e and f) . Moreover, the netic material actually afforded a higher degree of magnetic field reduction at a frequency of 600 kHz, as can be seen in Figure 6 g.

This important characteristic in the shielding data owes to the variation of the alloys permeability and conductivity with the frequency of the applied field , and this will be elaborated on in the following data analysis section. (Note that the effects of conductivity and permeability on the magnetic shielding capability of the netic and co-netic alloys is explained very elegantly in the application notes published by the Perfection Mica / Magnetic Shield Company)

It is also interesting to note that the " tin can " shield enclosures that were fabricated by the students could have afforded a higher degree of field attenuation if they had been covered with metal at both ends[2]. However , this would have prevented MaFEL laboratory measurements by the students because the highly attenuated field amplitudes would have been below the minimum detection sensitivity of the sensors (about 1.0 uT for the B-dot probe)

Incidentally, the presence of holes in a magnetic shield will allow the incident magnetic field to penetrate into the internal volume of the shield . [2] The amount of field leakage is a function of the hole size and the corresponding angle between the hole axis and incident flux lines .When the hole axis is perpendicular to the incident field, then the fringing field will extend approximately one hole diameter into the enclosure. When the hole axis is parallel to the impinging field, then the fringing field will extend about two hole diameters into the shielded enclosure. [2]

One more important lesson that the students were able to derive by carrying out the field measurements alluded to above was an enhanced understanding of the key differences between magnetic field shielding and the shielding of radio frequency (RF) electromagnetic waves . Although no specific measurements of RF electromagnetic fields or RF shielding effects are presently included in the MaFEL laboratory procedure, the aspect of shielding against interference caused by radio waves is worth discussing at this point in order to prevent confusion between RF shielding and the low frequency magnetic flux shielding that is the focus of the MaFEL procedure.

Magnetic shielding employs high permeability metals to divert undesired flux lines produced by an external source of low frequency (i.e. DC to < 100 kHz) magnetic field so that the flux lines are unable to couple into a sensitive electronic circuit. RF shielding involves the use of high conductivity metals, such as copper, to form a " screen room " in order to prevent traveling electromagnetic waves of radio frequencies (> 100 kHz) from coupling into a sensitive electronic circuit. The copper screen room shields the RF fields by the process of eddy current reflection, which is quite different from the process of concentrating magnetic flux lines in the shield material that is utilized in magnetic shielding. [1,2] Incidentally , the process of high frequency electromagnetic field shielding is discussed extensively in reference [1] .

The high permeability metals used for magnetic shielding can also function as RF shields, but they are not as effective as copper due to their lower conductivity. Conversely, copper or similar metals (e.g. gold, silver, platinum , aluminum) cannot be used as a magnetic shield owing to their low relative magnetic permeability of one.

Copyright @ 2005 , American Society for Engineering Education "

Performing the MaFEL experiment helps to reinforce the concepts of magnetic and RF shielding in the minds of the EET students and prepares them to devise effective solutions for both types of shielding design problems, if they should encounter them in their industrial careers.

To summarize , the data plots in Figures 4 and 6 depict the variation of the axial magnetic field amplitudes sensed by the probes over the 1 to 600 kHz range with and without magnetic shielding . In the following section, these graphs are analyzed and the engineering design information they convey is discussed.

IV. Analysis of Experimental Results

Inspection of the plots of field strength versus axial distance from the center of the wire loop (as seen in Figures 4 and 6) reveals that the field strength falls off in a quadratic manner with increases in distance, as was predicted by Eqn (2). The agreement between the data provided by the B-dot and commercial PM field probes is within 15 % at frequencies of 1 and 3 kHz, but falls off at higher frequencies due to the upper cutoff of 3 kHz for the calibrated frequency range of the PM probe . [2] The reasonably close agreement between the B-dot probe and the commercial sensor at the frequencies of 3 and 10 kHz attests to the good design calculations and craftsmanship displayed by the EET students when performing the MaFEL procedure. Further , the ability of the B-dot probe to accurately sense field intensities of increasing frequency right up to its parasitic LC resonance band of 250 kHz to 400 kHz also enhances the B-dot probes' value as a field monitoring instrument that can be used to evaluate electromagnetic shielding problems in electronic systems subjected to EMI for fields in the 60 Hz AC to the RF range .

Examination of the shielded field measurements made with the co-netic and netic " tin can "shields (as seen Figure 6) reveals the high degree of attenuation afforded by the use of such high permeability metals, even though one end of the " tin can " shield enclosure was left completely uncovered (which resulted in some leakage, as mentioned in Section III) .

The degree of attenuation for each of the alloys was calculated by dividing the unshielded field intensities by the field intensities that were measured when the probes were shielded. The shielding effectiveness was then expressed in decibels by multiplying the log of this attenuation ratio by 20 . The values of attenuation factor determined for the co-netic and netic shields at each frequency for both the B-dot and PM probes are listed in Table 4 . The attenuation observed for the netic alloy ranged from – 2.8 dB at 3 kHz to -14.4.dB at 100 kHz, while that for the co-netic alloy ranged from -7.5 dB at 3 kHz to -14.4 dB at 100 kHz ..

Perhaps the most fascinating aspect of the shielding data obtained for the co-netic and netic alloys is the merging of their attenuation factors for frequencies above 100 kHz. This owes to the rapid drop off of the alloy's relative permeability with frequency, which decays from 30000 (co-netic) or 600 (netic) at DC to about unity for both alloys at 100 kHz[2]. The reduction in relative permeability nullifies the prime mechanism of magnetic field shielding, which is to concentrate the incident magnetic flux lines into the space occupied by the high permeability shield metal so that the flux is diverted from the sensitive electronic circuit.

When the frequency of the incident field reaches the radio range (i.e. > 100 kHz), the optimum means of shielding such an RF electromagnetic field is by eddy current reflection. [1,2] In order to reflect an incident electromagnetic field effectively, the

Copyright @ 2005 , American Society for Engineering Education "

shielding metal requires a high conductivity. This explains why the netic shield actually provided greater attenuation at 600 kHz than the co-netic shield, because the higher conductivity of the netic metal is much more critical for shielding RF fields . (Recall that the relative permeability of both alloys drops to near unity for frequencies exceeding 100 kHz , so the process of magnetic flux line concentration in the metal no longer occurs and there is no attenuation of the incident field). [2] Of course, one of the traditional high conductivity metals, such as copper, galvanized steel or aluminum would offer a much greater degree of RF shielding than either netic or co-netic alloys and that is why the former metals are used for screened RF enclosures. [2]

In sum, the field measurement data plotted in Figures 4 and 6 illustrates the utility of using high permeability metals to shield against undesired coupling of low frequency AC magnetic fields into sensitive electronic systems. It also demonstrates the borderline in incident field frequencies where either magnetic or radio frequency shielding designs (and the use of correspondingly high permeability or high conductivity metals) must be implemented . For the shield metals that were featured in this paper, that frequency borderline was experimentally determined by the EET students to be around 100 kHz , as noted above . Thus the shielded and nonshielded field probe measurements that are included in MaFEL provide a valuable lesson in electromagnetics that the EET students can utilize in their careers, such as setting up computer controlled measurements in areas with intense EMI .

Table 4. The attenuation factor determined for the co-netic and netic shield alloys at the various test frequencies for the fields measured with the B-dot and PM probes at the center of the wire loop (i.e. z = 0) .

B-dot Probe: Frequency	Attenuation (co-netic)	Attenuation (netic)
3 kHz	-7.5 dB	-2.8 dB
10 kHz	-10.4 dB	- 4.4 dB
30 kHz	-12 dB	- 8.0 dB
100 kHz	-12.9 dB	-12.0 dB
200 kHz	-14.4 dB	-14.4 dB
600 kHz	-13.6 dB	-20.2 dB

PM Probe : Frequency	Attenuation (co-netic)	Attenuation (netic)
1 kHz	-7.9 dB	-2.6 dB
3 kHz	- 9.6 dB	- 2.6 dB
10 kHz	- 11 dB	- 3.7 dB

V. Conclusion

In conclusion , it can be stated that all aspects of the MaFEL procedure; including the design of the B-dot probe, the calibration of its sensitivity, and its use in the measurement of AC magnetic fields of variable frequency along the central axis of a wire loop ; provided a very comprehensive learning experience for the EET students in

Copyright @ 2005 , American Society for Engineering Education "

regards to electromagnetic induction, measurement of magnetic field distributions and the design / application of electromagnetic shielding systems . The data obtained by the students with their B-dot magnetic field sensors also correlated quite well with a commercial field detector , and the wider frequency range of the B-dot probe further attests to its utility as a viable laboratory instrument that an EET student can design and build for use in analyzing EMI problems . By performing the exercises engendered in the MaFEL laboratory procedures, the EET students gained valuable knowledge in electromagnetic principals that can assist them in effectively solving practical problems in electromagnetic shielding over the course of their professional careers.

This keener insight into electromagnetic induction, field mapping and shielding that EET students can gain by performing MaFEL , fills a critical void in the conventional EET curriculum (since no other courses in a conventional EET curriculum address these concepts in significant detail) .

As far as future development of the MaFEL laboratory experience is concerned, the EET faculty at Canton are making plans for students to use the B-dot probe in more complicated magnetic field geometries, such as the air gaps in rotational machinery or mapping the leakage flux produced by power transformers, and then comparing the measured field distributions to those calculated by commercial finite element analysis electromagnetic field plotting software , in order to correlate experiment and theory.

Moreover, the EET students may also be asked to design low noise solid state electronic amplifiers to interface with the B-dot probe in order to increase the probe sensitivity and facilitate computer controlled data acquisition. The foregoing represent just a few of the nearly unlimited educational projects for EET students (and their faculty) that the MaFEL procedure can evolve into.

VI. Acknowledgements

The authors wish to express their sincere appreciation to Professors R.E. Dollinger and W.J. Sarjeant of the Electrical Engineering Department at SUNY Buffalo, for it was their laboratory indoctrination exercises on electromagnetics for new EE graduate students that provided the author with the foundation that ultimately inspired the current work. Our appreciation for the many years of dedication, unlimited patience and goodwill shown by Dr. Dollinger and Dr. Sarjeant in the education and support of their graduate students will always be warmly remembered.

The authors are also pleased to note that the data appearing in Figures 4 and 6 of this paper was meticulously collected and analyzed by the EET students at SUNY Canton as part of their laboratory coursework .

REFERENCES

[1] Applied Electromagnetics , Martin A. Plonus, McGraw Hill Book Co., New York, 1978 .

[2] Magnetic Shield / Perfection Mica Corporation, Catalog no. RE-2@2004, 740 N. Thomas Drive, Bensenville, IL 60106 .

[3] Radio Engineers Handbook, F.E. Terman, McGraw Hill Book Co., New York, 1943.

Copyright @ 2005 , American Society for Engineering Education "